Textile UWB Antennas for Wireless Body Area Networks

Maciej Klemm, *Member, IEEE*, and Gerhard Troester, *Senior Member, IEEE*

***Abstract*—A new ultrawideband (UWB) textile antenna designed for UWB wireless body area network (WBAN) applications is presented. Unlike previous textile antennas, these antennas offer a direct integration into clothing due to a very small thickness (0.5 mm) and flexibility. We have realized two different designs of textile antennas: coplanar waveguide fed printed UWB disc monopole and UWB annular slot antenna. To our knowledge, these are the first textile UWB antennas reported in the open literature. Measured return loss and radiation pattern characteristics of textile UWB antennas agree well with simulations. Moreover, measured transfer functions show that these textile antennas possess excellent transient characteristics, when operating in free space as well as on the human body. They can operate in the entire UWB band approved by the Federal Communications Commission (3.1–10.6 GHz).**

***Index Terms*—Body area networks, textile antennas, ultrawideband (UWB).**

I. Introduction

WEARABLE computing is a new, fast growing field in application-oriented research [1]. Steadily progressing miniaturization in microelectronics along with other new technologies enables wearable computing to integrate functionality in clothing allowing entirely new applications. In this sense, wearable computing can be seen as a part of the wireless body area network (WBAN) [2]. Integration in textiles ideally combines the requirements of wearable computing (and WBANs), since clothing is unobtrusive and offers large area and close body proximity. However, such electronic devices have to meet special requirements concerning wearability.

Ultrawideband (UWB) is an emerging wireless technology, recently approved by the Federal Communications Commission (FCC). In low/medium data-rate applications, like wearable computing, UWB offers low-power operation and extremely low radiated power, thus being very attractive for body-worn battery-operated devices.

In this paper, we present new UWB textile antennas for wearable applications. The originality of this paper lies with new textile implementations of UWB wearable antennas; no new fundamental antenna theory is addressed. Our new antennas are made entirely of textiles. Previous textile antennas were usually composed of dielectric materials with ϵ_r only slightly higher than one, and thicknesses of 4–8 mm [3], [4]. A new feature of our UWB textile antennas is that they could be easily integrated directly into clothing, rather than being attached, since they are only 0.5 mm thick. We have realized different types of thin UWB textile antennas, both in microstrip and coplanar waveguide (CPW) techniques. To the best of our knowledge, these are the first CPW-fed textile antennas reported in the open literature.

This paper is organized as follows. In Section II, we describe textile materials used for antenna manufacturing and the manufacturing process. In Section III, we present two different UWB textile antennas, together with measured and simulated return loss and radiation patterns characteristics. Section IV compares the pulsed characteristics (transfer function, radiated/received pulses) of the textile UWB annular slot antenna with its counterpart realized using typical microwave substrate and metal etching. Next, we present the human body influence on transient characteristics of the textile UWB antenna, when mounted at different distances from the body. Conclusions are drawn in Section V.

II. Textile Materials and Antennas Manufacturing

A. Textile Materials

As a conductor, we have used high conductive metallized Nylon fabric—*Nora*.[1] Its three metallized layers (Ni/Cu/Ag) provide high conductivity (surface resistivity of 0.03 Ω/square) and protection against corrosion, as well as extreme flexibility. For our textile antennas, we chose an acrylic fabric 0.5 mm thick as a dielectric substrate. Such a substrate possesses several advantages compared to other fabrics. It is light with good drapability while being dimensionally stable in height. We used techniques explained in [5] in order to extract the permittivity of the textile substrate. This technique utilizes S-parameter measurements of two transmission lines of different lengths. Knowing the length difference and the S-parameters, a permittivity of 2.6 +/− 0.1 between 3 and 10 GHz was extracted for the acrylic textile.

The thickness of the dielectric is not only important for easy integration with clothing but should also provide the possibility to realize a feeding transmission line of an appropriate characteristic impedance (in our case 50 Ω). This is an important issue in the design of textile antennas.

B. Manufacturing

In the manufacturing process, the attachment of the conductive textile to the substrate turns out to be very critical. First of all, the dimensions of an antenna must be retained while being attached to the substrate. Secondly, the adhesive for composition must not affect the electrical properties of textile materials, e.g., the sheet resistance of the conductive textile. The adhesive

Manuscript received September 16, 2005; revised April 3, 2006.

The authors are with the Electronics Laboratory, Department of Information Technology and Electrical Engineering, Swiss Federal Institute of Technology Zürich, 8092 Zürich, Switzerland (e-mail: klemm@ife.ee.ethz.ch).

Color versions of Figs. 1(a), 3(a), 6, and 7 are available online at http://ieeexplore.ieee.org.

Digital Object Identifier 10.1109/TAP.2006.883978

[1]http://www.shieldextrading.com/images/pdfs/nora.pdf.

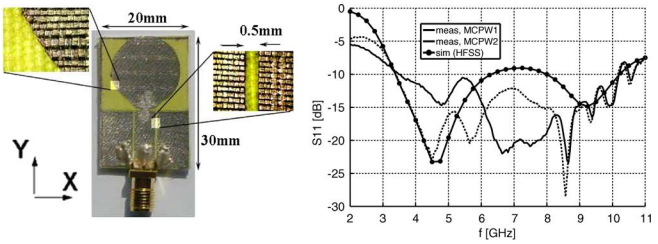

(a) (b)

Fig. 1. CPW-fed textile UWB disc monopole antenna: (a) photograph and (b) measured and simulated return loss characteristics. MCPW1, MCPW2: two prototypes of this textile antenna.

sheets turned out to be a good solution as they evenly deposit as thin layer on the conductive textile by ironing. Moreover, adhesive penetrates only the surface of the conductive textile, such that sheet resistance and permittivity are not changed. The electrical connection to a subminiature version A (SMA) jack was established with conductive two-component glue. Antenna and transmission lines for extraction of permittivity were constructed in the same manner.

III. Antenna Design

All UWB antennas presented in the following were designed to operate in the entire UWB band approved by the FCC, from 3.1 to 10.6 GHz. Commercially available electromagnetic solver Ansoft HFSS was used during design. As the design criterion, we looked at the return loss (RL) characteristics. From many antennas suitable for UWB communication, we chose those offering low profile and small size, as this also makes them attractive for use in WBAN.

A. CPW-Fed Textile UWB Disc Monopole

We have designed and realized the UWB disc monopole antenna, fed by the coplanar line [Fig. 1(a)]). CPW feeding technique offers uniplanar antenna structures that can be of advantage, e.g., if one would use printing-on-textile process for realization of an antenna pattern. Uniplanar structure also eliminates all problems associated with the alignment of different conductive layers. But CPW feeding also has disadvantages that are even more pronounced when applied to the textile transmission lines. Namely, to realize the characteristic impedance of 50 Ω, and with reasonable width of a central CPW conductor, one needs to realize a small gap between central line and ground plane. As is easy to imagine, this is a problem in case of a textile conductor, since only a simple cutting tool (e.g., a scalpel) is used, and the definition of conductor edges is not precise (depending on the material used). With our dielectric, we managed to realized 0.5 mm gap between conductors [see zoom region in Fig. 1(a)], which with the 4.8 mm width of the central line resulted in the impedance of 59 Ω. Fig. 1(b) presents a comparison between measured and simulated RL characteristics. We can see higher RL variation when comparing the two CPW textile prototypes (CPW1 and CPW2) to microstip-fed antennas. Also agreement with simulated results is worse. These discrepancies can mostly be related to manufacturing problems. Since the antenna is composed of several pieces of the conductive textile, it is not easy to insure all dimensions are correct during the attachment to the dielectric.

To show that these antennas are still reasonably good, in Fig. 2 we present comparison between measured and simulated radiation patterns at 3.1, 6, and 9 GHz for two major cut-planes: XZ and YZ. We can clearly see that results agree well, and small discrepancies are within an acceptable level.

B. Microstrip-Fed Textile UWB Annular Slot

The last antenna we present is the UWB annular slot antenna, fed by a short microtrip line [Fig. 3(a)]. The radiating slot was realized with the use of two conductive layers. The planar antenna size is 30×30 mm^2. Fig. 3(b) presents a comparison between measured and simulated RL characteristics. All antennas have good input matching, and the measured and simulated results agree well. Again, small discrepancies can be associated with antenna manufacturing and connections. Comparing two textile antenna prototypes S1 and S2, we can see that return loss characteristics are very close: the biggest difference occurs between 9 and 10 GHz. In Fig. 4, we compare measured and simulated radiation patterns at 3.1, 6, and 9 GHz for two major cut-planes XZ and YZ. Besides the pattern in the XZ plane at 9 GHz [Fig. 4(c)], where the difference is rather significant, simulated and measured patterns show good agreement.

IV. UWB Antenna Characterization

A. Parameters

In the previous section, we presented return loss and radiation pattern results, which are usually used in the assessment of antenna performance. In the case of UWB systems however, frequency-domain transfer function (TF) is the most important measure [7], [8]. It not only allows direct examination of broadband performance in the frequency domain but also gives an insight into the time domain when inverse Fourier transform is applied. Generally, we can define three transfer functions for a single antenna [9]: 1) H_{Tx}—transmit (Tx) transfer function, 2) H_{Rx}—receive (Rx) transfer function, and 3) H_{2ant}—transfer function when the same antenna is used in the Tx and Rx mode. These functions are defined as [9] $H_{Tx}(\omega,\theta,\phi) = E_{\mathrm{rad}}(\omega,\theta,\phi)/V_{in}(\omega)$, $H_{Rx}(\omega,\theta,\phi) = V_{\mathrm{load}}(\omega,\theta,\phi)/E_{\mathrm{inc}}(\omega,\theta,\phi)$. H_{Tx} and H_{Rx} are the transmit- and receive-transfer functions, relating the radiated electric field intensity $\mathrm{E_{rad}}$ to the antenna driving waveform V_{in}, and the received voltage on the (complex) load $\mathrm{V_{load}}$ to the incident electric field $\mathrm{E_{inc}}$, respectively. Both transfer functions include antenna matching characteristics. Tx and Rx transfer functions are related by: $\mathcal{H}_{Tx}(\omega,\theta,\phi) = j\omega H_{Rx}(\omega,\theta,\phi)$. The term $j\omega$ is therefore the factor describing the antenna reciprocity relationship in a transmit and receive mode. Therefore complete transfer function for the system of two identical antennas H_{2ant}, relating a voltage across the receiver load with the pulse exciting the Tx antenna, has the form $H_{2ant}(\omega,\theta,\phi) = H_{Tx}(\omega,\theta,\phi) \cdot H_{ch}(\omega,\theta,\phi) \cdot H_{Rx}(\omega,\theta,\phi) = S_{21}$. H_{ch} stands for the propagation channel. If measurements are performed in the anechoic chamber, we can assume $|\mathrm{H}_{ch}| = 1$. For us it is important to notice that H_{2ant} is equal to the S_{21} scattering parameter.

B. Measured H_{2ant} Transfer Functions

In the following we present the measured S_{21} characteristics of the UWB annular slot antenna, in the textile version

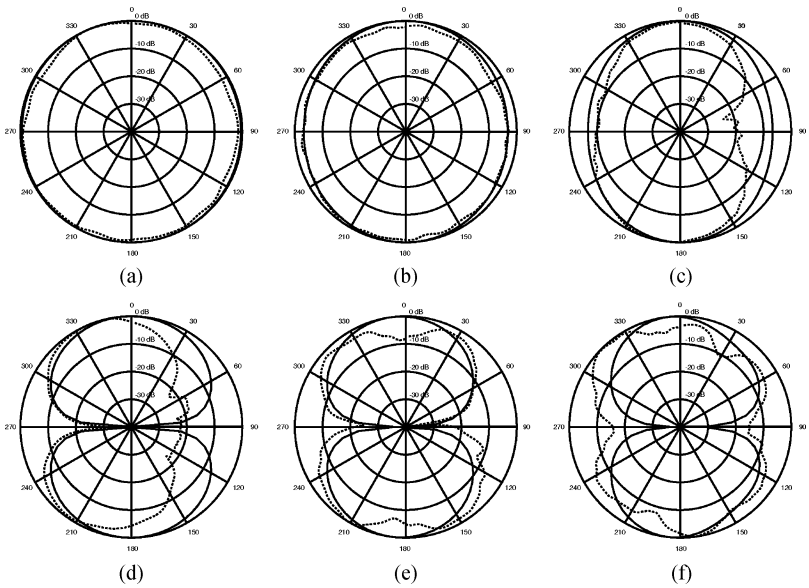

Fig. 2. Comparison of measured and simulated radiation patterns of the CPW-fed UWB monopole antenna: (a) XZ plane 3.1 GHz, (b) XZ plane 6 GHz, (c) XZ plane 9 GHz, (d) YZ plane 3.1 GHz, (e) YZ plane 6 GHz, and (f) YZ plane 9 GHz.

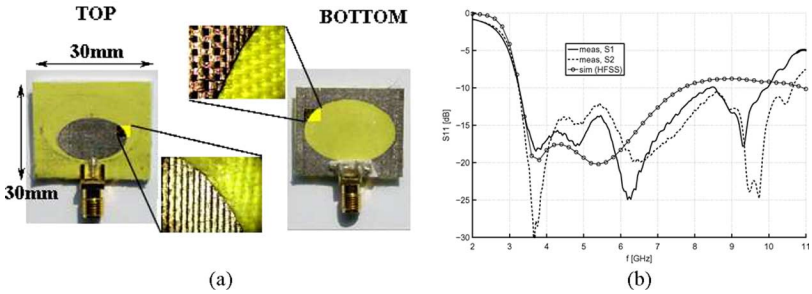

Fig. 3. Microsrip-fed textile UWB annular slot antenna: (a) photograph and (b) measured and simulated return loss characteristics. S1, S2: two prototypes of this textile antenna.

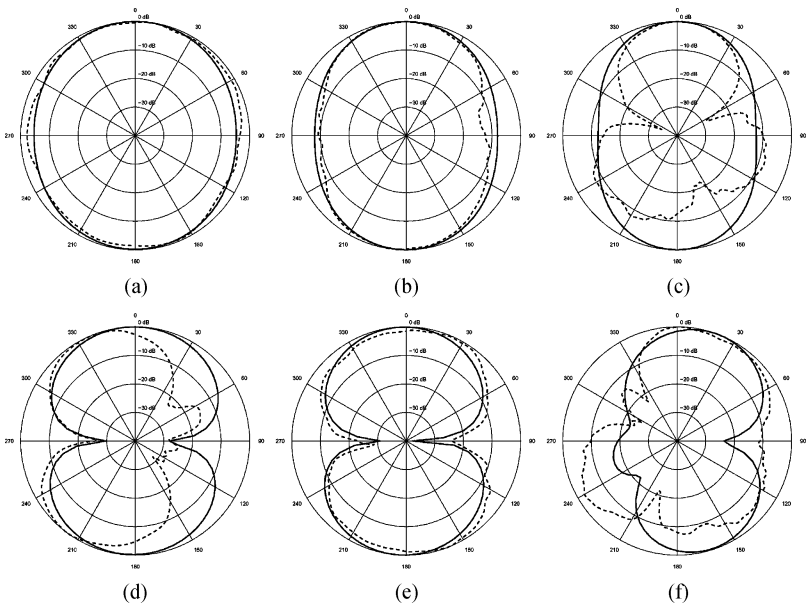

Fig. 4. Comparison of measured and simulated radiation patterns of the textile UWB annular slot antenna: (a) XZ plane 3.1 GHz, (b) XZ plane 6 GHz, (c) XZ plane 9 GHz, (d) YZ plane 3.1 GHz, (e) YZ plane 6 GHz, and (f) YZ plane 9 GHz.

(see Section V), and its counterpart realized using conventional etching and a microwave substrate (0.5 mm thick, Rogers 3003). The reference antenna (abbreviated PCB) has the same geometry as the textile antenna. The goal of this measurement was

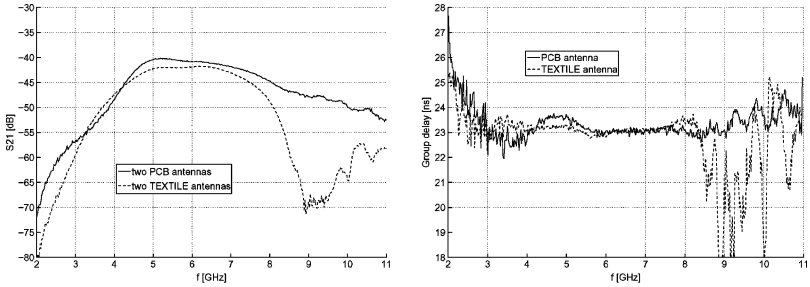

(a) (b)

Fig. 5. Measured H_{2ant} transfer functions (S21) of the PCB and textile UWB annular slot antennas: (a) magnitude and (b) group delay.

twofold: to assess transient characteristics of the UWB textile antenna and to compare the transient performance of the antennas designed in the textile and traditional technology.

Results are presented in Fig. 5 for a distance of 1 m between Tx and Rx antennas located in an anechoic chamber. Two antenna types, PCB and textile antennas, were measured, with a pair of antennas facing each other in the direction of maximum radiation (0° in Fig. 4). We can see that up to 7 GHz, the magnitude of S_{21} [Fig. 5(a)] is comparable for the PCB and textile antenna, slightly lower (about 1 dB) for the latter one. But within the 8–11 GHz band, there is a clear difference between these antennas. As the measured RL did not indicate a possible discrepancy, the fall in the amplitude of S_{21} could be due to losses and also a shift in the radiation pattern. From Fig. 5(b) we can see that the group delay (defined as $\tau = -d\phi/df$, $\phi-\mathrm{S}_{21}$ phase) varies significantly above 8.5 GHz for the textile antenna. Between 3 and 8.5 GHz both antennas have a flat group delay, indicating good transient response.

C. Transmitted Pulses

In this section, we compare transient characteristics of the *PCB* and *textile* UWB annular slot antennas by examining transmitted UWB pulses. To do so, we assume three different pulses as an excitation. As an antenna excitation waveform, a modulated Gaussian pulse was chosen due to the close-form mathematical expression of the following form:

$$s(t) = e^{-((t-a\cdot\tau)/\tau)^2} \cdot sin\left(2\pi f_r \cdot (t - a\cdot\tau)\right). \qquad (1)$$

In calculating transmitted waveforms (based on measured S_{21}), we have assumed three different input pulses:

a) $\mathrm{f}_c = 4.5$ GHz, $\tau = 210$ ps, $\mathrm{a} = 3$ (called *Pulse1* later on);
b) $\mathrm{f}_c = 6$ GHz, $\tau = 110$ ps, $\mathrm{a} = 4$ (*Pulse2*);
c) $\mathrm{f}_c = 6$ GHz, $\tau = 60$ ps, $\mathrm{a} = 4$ (*Pulse3*).

Their voltages and respective spectra are presented in Fig. 6.

Desired transient responses were obtained numerically, by multiplying the spectra of the respective input pulse and the transfer function $(\mathrm{H}_{2ant} = \mathrm{S}_{21})$. An inverse Fourier transform was then applied to obtain transmitted pulse.

In Fig. 7, we present transmitted pulses using a pair of PCB and a pair of textile antennas. We can clearly see how the transfer function influences waveforms of received pulses. Since both antennas have almost the same characteristics below 7 GHz, we can also see that with Pulse1 as the excitation, the pulses received [Fig. 7(a)] are almost exact replicas. For shorter pulses

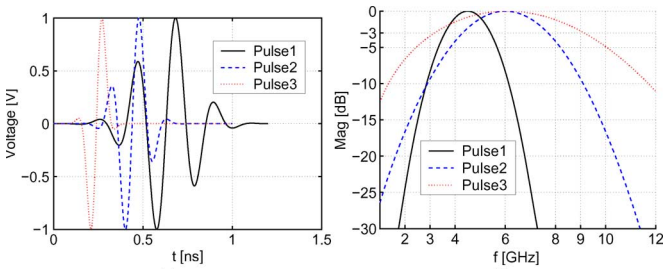

(a) (b)

Fig. 6. Different excitation pulses: (a) time domain waveforms and (b) spectra.

(Pulse2, Pulse3) with a significant energy content at higher frequencies (>6 GHz), we can see that resulting waveforms have lower amplitude for the textile antenna, as one would expect from the shape of the transfer function. But all pulses still have similar shape and comparable duration. Quantitatively, pulses for the *PCB/textile* antenna have duration of 599/558, 322/356, and 235/316 ps, assuming that the Tx antenna is excited using Pulse1, Pulse2 and Pulse3, respectively. Pulse duration is defined as the time window with 99% of the total pulse energy. Comparing shape, fidelity values are 99%, 98%, and 96%. Fidelity is defined as

$$F = max\frac{\int_{-\infty}^{\infty} x(t)\cdot y(t-\tau)dt}{\sqrt{\int_{-\infty}^{\infty}|x(t)^2|\,dt\cdot\int_{-\infty}^{\infty}|y(t)^2|\,dt}}. \qquad (2)$$

D. On-Body Characteristics of the Textile UWB Annular Slot Antenna

In this section, we investigate the influence of the human body on performance of the textile UWB annular slot antenna. We have measured the H_{2ant} (S_{21}), when the Tx antenna was mounted on the human body (chest) and the Rx antenna was kept in free space, 0.5 m away. The Tx antenna was mounted at three different distances to the body: 2, 4, and 6 mm. These measurements were performed in the office room (unlike measurements from Section III-B and III-C, done in the anechoic chamber), to approximate more realistic operational scenarios. Measurement of the H_{2ant} in free space was done for comparison and the results are shown in Fig. 8(a). First, we see that due to the indoor environment $(H_{ch} \neq 1)$, the free space H_{2ant} transfer function is slightly different than that presented in Fig. 5(a) (measurement in the anechoic chamber).

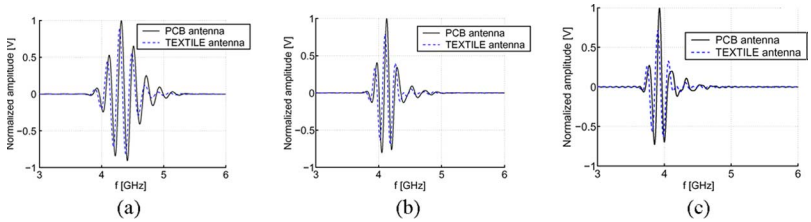

Fig. 7. Received pulses (two-antenna system) for different excitations: (a) Pulse1, (b) Pulse2, and (c) Pulse3.

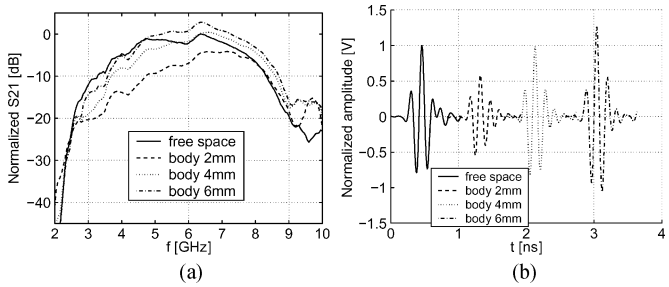

Fig. 8. On-body characteristics of the textile UWB annular slot antenna: (a) H_{2ant} transfer functions and (b) transmitted pulses (Pulse3 as an input pulse). Results are shown for three different distances between the antenna and body (2, 4, 6 mm).

When the Tx antenna is mounted 2 mm away from the human body, we observe significant (up to 9 dB) drop in $|\mathrm{H}_{2ant}|$ between 3 and 8 GHz, compared with the free space case. Above 8 GHz, free space and on-body characteristics are comparable. When we increase the separation between the Tx antenna and the body, we observe that $|\mathrm{H}_{2ant}|$ below 6 GHz is 2–3 dB lower compared to free space. Above 6 GHz it exceeds (by 1–2 dB) the amplitude of S_{21} in free space. This trend continues as the separation between the antenna and body increases. At 6 mm distance, we can see that above 4.7 GHz, the amplitude of the on-body transfer function is higher compared to the free space case. These results indicate that the human body is strongly reflecting EM waves at high frequencies (>4.5 GHz), if the antenna's near fields do not significantly extend into the human body.

Based on measured transfer functions, we have calculated the transmitted pulses between on-body Tx antenna and Rx antenna in free space, assuming Pulse3 as the excitation. Results are presented in Fig. 8(b). We can see that the human body did not significantly change either the shape (fidelities >95%) or the duration of transmitted pulses (270 ps for free space, 310–320 ps for on-body case). The only clearly visible change is the energy of pulses. Assuming the energy of the pulse transmitted in free space as 100%, the pulses for on-body scenarios have energies of 35, 98, and 163% for distances of 2, 4, and 6 mm, respectively.

V. Conclusions

A number of new textile UWB antennas for WBAN applications have been presented in this work. Unlike prior textile antennas, these antennas offer a direct integration into clothing due to a very small thickness (0.5 mm) and flexibility. In the designed textile antennas we have used microstrip as well as coplanar feeding lines. Measured return loss and radiation pattern characteristics of textile UWB antennas agree reasonably well with simulations. Measured transfer functions show that UWB textile antennas possess excellent transient characteristics, comparable to the counterpart PCB realization. We have shown that it is possible to transmit very short UWB pulses with textile antennas. These results were achieved by the proper choice of textile materials, as well as design. But the manufacturing of textile antennas is the critical step, in order to obtain good performance. To achieve a good repeatability of textile antennas, more advanced manufacturing methods should be employed. Our results constitute a further step towards the realization of a system-on-textile vision and UWB wireless body area networks.

Acknowledgment

The authors are grateful to H. Benedickter, IFH, for great help with antenna measurements. They would like also to thank F. Trösch, Wireless Communication Group, ETHZ, for fruitful discussions concerning signal processing.

References

[1] T. E. Starner, "Wearable computing for the developing world," *IEEE Pervasive Comput.*, vol. 4, pp. 87–91, Jul.–Sep. 2005.

[2] T. Zasowski, F. Althaus, M. Stäger, A. Wittneben, and G. Tröster, "UWB for noninvasive wireless body area networks: Channel measurements and results," presented at the IEEE Ultra Wideband Syst. Technol. Conf. (UWBST 2003), Reston, VA, Nov. 2003.

[3] M. Klemm, I. Locher, and G. Troster, "A novel circularly polarized textile antenna for wearable applications," in *34rd Eur. Microwave Conf. (EuMC)*, Amsterdam, The Netherlands, Oct. 11–14, 2004.

[4] P. Salonen, Y. Rahmat-Samii, and M. Kivikoski, "Wearable antennas in the vicinity of human body," in *IEEE Antennas Propag. Society Symp.*, Jun. 20–25, 2004, vol. 1, pp. 467–470.

[5] J. Grzyb, I. Ruiz, and G. Troster, "An investigation of the material and process parameters for thin-film MCM-D and MCM-L technologies up to 100 GHz," in *Proc. 53rd Electron. Comp. Technology Conf. (ECTC 2003)*, New Orleans, LA, May 2003, pp. 478–486.

[6] J. Liang, C. C. Chiau, X. Chen, and C. G. Parini, "Printed circular disc monopole antenna for ultra-wideband applications," *Electron. Lett.*, vol. 40, no. 20, pp. 1246–1247, Sep. 30, 2004.

[7] Z. N. Chen, X. H. Wu, H. F. Li, N. Yang, and M. Y. W. Chia, "Considerations for source pulses and antennas in UWB radio systems," *IEEE Trans. Antennas Propag.*, vol. 52, no. 7, pp. 1739–1748, Jul. 2004.

[8] X. H. Wu and Z. N. Chen, "Design and optimization of UWB antennas by a powerful CAD tool: PULSE KIT," presented at the IEEE Antennas Propag. Soc. Symp., Jun. 20–25, 2004.

[9] D. Lamensdorf and L. Susman, "Baseband-pulse-antenna techniques," *IEEE Antennas Propag. Mag.*, vol. 36, pp. 20–30, Feb. 1994.

Maciej Klemm (M'03) was born in 1978. He received the M.Sc. degree in microwave engineering from Gdansk University of Technology, Poland, in 2002. He is currently pursuing the Ph.D. degree at the Electronics Laboratory, Swiss Federal Institute of Technology Zurich, Switzerland.

His current research interests include small UWB antennas and UWB communications, antenna interactions with a human body, electromagnetic simulations, microwave MCM technologies, and millimeter-wave integrated passives (European IST LIPS project). In spring 2004, he was a Visiting Researcher at the Antennas and Propagation Laboratory, University of Aalborg, Denmark, where he was working on new antennas for UWB radios.

Mr. Klemm received the Young Scientists Content award at IEEE MIKON 2004 for a paper about antennas for UWB wearable radios. He is a Reviewer for the IEEE TRANSACTIONS ON ANTENNAS AND PROPAGATION.

Gerhard Tröster (SM'93) received the M.S. degree from the Technical University Karlsruhe, Germany, in 1978 and the Ph.D degree from the Technical University of Darmstadt, Germany, in 1984, both in electrical engineering.

He is a Professor and Head of the Electronics Laboratory, Swiss Federal Institute of Technology Zürich, Switzerland. During the eight years he spent with Telefunken Corporation, Germany, he was responsible for various national and international research projects focused on key components for ISDN and digital mobile phones. His field of research includes wearable computing, reconfigurable systems, signal processing, mechatronics, and electronic packaging. He has authored and coauthored more than 100 paper and has received five patents. In 1997, he cofounded the spinoff u-blox AG.